Frontiers in Heat and Mass Transfer (FHMT), 14, 28 (2020)
DOI: 10.5098/hmt.14.28

Global Digital Central
ISSN: 2151-8629

Frontiers in Heat and Mass Transfer

Available at www.ThermalFluidsCentral.org

ROLE OF MAXWELL VELOCITY AND SMOLUCHOWSKI TEMPERATURE JUMP SLIP BOUNDARY CONDITIONS TO NON-NEWTONIAN CARREAU FLUID

T. Sajid†, M. Sagheer , S. Hussain

Capital University of Science and Technology, Islamabad, 46000, Pakistan

ABSTRACT

The forthright aim of this correspondence is to examine the conduct of MHD, viscous dissipation and Joule heating on three dimensional non-Newtonian Carreau fluid flow over a linear stretching surface. Impact of non-linear Rosseland thermal radiation and homogenous/heterogenous reaction process have been also considered to examine the heat and mass transfer process during fluid flow. The velocity and thermal slip effect at the surface have also been scrutinized in detail. By utilizing a suitable transformation, the modelled partial differential equations (PDEs) are renovated into ordinary differential equations (ODEs) and furthermore solved with the help of the numerical procedure namely the RK-4 method embedded with shooting procedure. The behaviour of the velocity, temperature and concentration profiles against various parameters are portrayed in the form of figures and tables. In the presence of the Maxwell velocity slip effect, the velocity profile is found to diminish. It is experienced that the temperature profile depreciates as a result of an augmentation in the Smoluchowski temperature slip effect and moreover concentration profile depreciates as a result of an improvement in the homogeneous and heterogeneous reaction parameters. To affirm the reliability of the proposed numerical technique, a comparison with already published work is also taken into account. A remarkable agreement amongst the accomplished and the existing outcomes has been obtained.

Keywords: *Nonlinear thermal radiation, viscous dissipation, velocity slip, temperature slip, homogenous/heterogenous reaction.*

1. INTRODUCTION

During the past two decades, widespread interest is developed in researchers to analyze the fluid flow behaviour and energy transfer phenomenon in the non-Newtonian fluid models like Bingham, power-law, Ellis, Casson, Eyring-Powell and Carreau fluid models. Examples of non-Newtonian fluids are ketchup, genetic liquids, shampoo, blood , tooth paste etc. Nagalakshm and Vijaya (2020) scrutinized the impact of MHD on Carreau nanofluid past a nonlinear stretching sheet. Their main finding was that an augmentation in magnetic parameter force guides to an abatement in the velocity profile. Cortell (2011) studied the impact of the power-law fluid flow towards an elastic porous stretching sheet embedded with the inclusion of effects like suction, thermal radiation and viscous dissipation. He observed that the thermal boundary-layer thickness diminishes on the account of an increment in the thermal radiation parameter. Ghiasi and Saleh (2019) scrutinized the two dimensional Casson fluid past a stretching sheet by incorporating the effects of Joule heating and non-uniform heat source/sink. They concluded that the temperature field augments by rising the Eckert number. Ali and Sandeep (2017) studied the MHD Casson-ferro fluid with the aid of effect like nonlinear thermal radiation and found that the nonlinear thermal radiation is the major factor responsible for regulation of the temperature at the thermal boundary layer. Three dimensional fluid accompanied with variable thermal conditions for the case of stretching surface was scrutinized by Liu and Andersson (2008) with the conclusion that the Nusselt number decreases by rising the internal heat parameter. Hayat *et al.* (2017) pondered three dimensional nanofluid flow over a stretching sheet accompanied with heat and mass flux boundary conditions. Khan *et al.* (2017a) studied the behaviour of 3D magneto Carreau nanofluid past a stretching sheet. They observed that by enhancing the magnetic parameter, a decrement in the velocity gradient is resulted. Megahed (2019) studied the impact of variable thermal conductivity and thermal radiation on Carreau fluid past a nonlinear stretchable surface. Raju and Sandeep (2016) investigated the impact of MHD, nonlinear thermal radiation and heat source/sink on unsteady Carreau fluid moving over a stretching sheet. To learn a bit more about the discussed issues, some more relevant articles are cited in Turkyilmazoglu (2014); Mukhopadhyay *et al.* (2013); Misra and Adhikary (2017); Narayana *et al.* (2014); Azam *et al.* (2017); Olajuwon (2011); Machireddy and Naramgari (2018).

Thermal radiation is actually an electromagnetic radiation produced by the thermal motion of particles in matter. These radiations actually move in the form of electromagnetic waves like those from electric burner and room heater. Thermal radiation has immense applications in agriculture, space exploration, law enforcement, polymer preparation, furnace design, electricity generation etc. The linear thermal radiation can be achieved by linearizing the Rosseland approximation and furthermore linear thermal radiation has unique Prandtl number Magyari and Pantokratoras (2011). The problem with linear thermal radiation is that it looses its effectiveness at high temperature difference. To overcome this obstacle, researchers recently introduced the nonlinear thermal radiation. The temperature becomes highly nonlinear in the occurrence of nonlin-

† *Corresponding author. Email: tanveer.sajid15@yahoo.com*

Global Digital Central
ISSN: 2151-8629

ear thermal radiation. In the case of nonlinear thermal radiation three key factors Prandtl number, temperature ratio parameter and thermal radiation are responsible for heat transfer analysis. Nonlinear thermal radiation has been applicable where high temperature difference is required and has distinguished applications in high temperature energy sector like polymer production, thermal furnaces, nuclear reactor, space craft etc. Impact of nonlinear thermal radiation and activation energy on Maxwell nanofluid past a stretchable surface have been debated in detail by Sajid *et al.* (2018). Magyari and Pantokratoras (2011) studied the impact of linear thermal radiation on various boundary layer flows. The only parameter which is helpful to linearize the Rosseland approximation is the radiation parameter. Krishnamurthy *et al.* (2016) studied the impact of nonlinear thermal radiation on water based nanofluid accompanied with slip effects. They perceived that the velocity profile diminishes by rising the velocity slip parameter. Astuti *et al.* (2019) contemplated the impact of thermal radiation on nanofluid past a variable stretchable surface and observed that an amplification in radiation parameter guides to a augmentation in the temperature field. Mohamed and Wahed (2017) studied the impact of nanoparticles, MHD and nonlinear Rosseland thermal radiation on a continuously moving surface. They observed that the Nusselt number rises by enhancing the radiation parameter. Cortell (2014) pondered the impact of thermal radiation on the fluid flow over a stretching surface. It was established that the temperature profile embellishes for the larger values of the temperature ratio parameter but behaviour is quite opposite in the case of thermal radiation parameter. Mahanthesha *et al.* (2016) delineated the water based nanofluid flow over a stretching surface with the combination of effect like nonlinear thermal radiation and canvassed that the nonlinear thermal radiation has higher impact on the flow field as compared to the linear thermal radiation. The impact of variable thermal conductivity and viscous dissipation on radiative fluid past a stretching sheet was investigated by Shateyi and Muzara (2020) with the conclusion that the temperature profile upsurges because of an escalation in the radiation parameter. The impact of nonlinear thermal radiation on 3D Carreau fluid past a stretchable surface was investigated by Khan *et al.* (2017b). The influence of nonlinear thermal radiation and bio-convection on Carreau fluid was deeply investigated by Raju et al. Raju *et al.* (2016). Jyothi and Reddy (2019) studied the effect of magnetite nanoparticles and zero mass flux boundary condition on radiative Carreau fluid past a stretching sheet.

A catalyst is a substance which speeds up the chemical reaction without itself being consumed. Catalysts are categorized into two types namely the homogeneous and the heterogeneous catalysts. In case of the homogenous reaction, the catalyst and the reactant are in same phases both are solids or liquids, but reverse in the case of heterogenous reaction where both occur in the different phase (one is solid other is liquid). Different chemical reaction structures involve homogenous/heterogenous reactions like polymer production, biochemical systems, combustion and catalysis. Ziabakhsh *et al.* (2010) investigated a steady incompressible fluid along with chemically reactive species past a porous stretching sheet. Kameswaran *et al.* (2013) studied the dynamics of a fluid past a porous stretching sheet with the inclusion of nanoparticles and chemical reaction and claimed that the temperature field decreases with an enrichment in the Weissenberg number. Merkin (1996) considered the model over a boundary flow with homogeneous/heterogeneous reaction. Nandkeolyar *et al.* (2014) contemplated a viscous incompressible fluid flow past a stretching surface under the effects of homogeneous/heterogeneous reaction and MHD. They deliberated that an augmentation in the magnetic field parameter guides to a decrement in the velocity profile. Bilal *et al.* (2017) observed the behaviour of non-Newtonian Williamson fluid past a stretching cylinder under the effect of stagnation point, homogeneous/heterogeneous reaction and MHD. Mansur *et al.* (2016) pondered a fluid past a stretching surface with the inclusion of nanoparticles and homogeneous/heterogeneous reaction phenomenon and found a reduction in the mass fraction due to an increment in the homogeneous/heterogeneous reaction parameter. The behaviour of Casson-Carreau fluid in addition to homogeneous/heterogeneous reaction is inspected by Gireesha *et al.* (2017) with the main finding that the temperature profile boosts up by mounting the temperature ratio parameter. Bachok *et al.* (2011) explored the effect of a stagnation point flow on the fluid flow over a stretching sheet combined with homogeneous/heterogeneous reaction and came up with the conclusion that a variation in the heterogeneous reaction parameter brings about a diminishment in the concentration profile. Chaudhary and Merkin (1995) considered a simple isothermal model with the inclusion of homogeneous/heterogeneous and stagnation point. Irfan *et al.* (2018) scrutinized Carreau fluid past a stretching sheet embedded with homogeneous/heterogenous reaction, variable thermal conductivity and heat source sink. The impact of homogeneous/heterogenous reaction on 3D Carreau fluid past a stretchable sheet was discussed by Khan *et al.* (2018).

In recent years, various researchers investigated the behaviour of the slip boundary layer phenomenon over different types of surfaces. The velocity of the fluid tends to zero and no surface friction takes place with regard to no slip condition, but in the case of slip condition, the fluid velocity normal to the wall is zero whereas its tangential velocity is non-zero. The slip conditions are considered important to study the micro-elastic mechanical systems, artificial heart cell etc. It is experienced that by including the velocity slip condition at the boundary, the heat transfer rate is increased. Recently, Aljoufi and Ebaid (2016) scrutinized a fluid flow towards a stretchable surface along with slip effects. They determined that the temperature profile diminishes by augmenting the slip parameter and Biot number. Zheng *et al.* (2012) scrutinized the viscous fluid flow towards a stretchable surface along with the velocity slip condition. They profound that the mass transfer rate upsurges by mounting Prandtl number. The effects of slip conditions, binary chemical reaction on stagnation point flow in a porous medium with convective boundary condition are considered by Sivasankaran *et al.* (2017). They concluded that an enrichment in the chemical reaction parameter reduces the heat transfer rate. Devakar *et al.* (2014) scrutinized the couple stress fluid between parallel plates with inclusion of slip effects. They perceived that the velocity in the couette flow is enhanced when the lower and the upper plates move in the same direction. The effects of nonlinear velocity slip over a stretching permeable surface is deliberated by Xinhui *et al.* (2017). They determined that the boundary layer thickness of velocity becomes thinner by rising the magnetic field parameter. Fang *et al.* (2009) deliberated the MHD viscous fluid flow over a stretching sheet in the presence of the slip effect. They analyzed that the wall slip velocity boosts in the case of an improvement in the magnetic parameter. The behaviour of velocity slip, thermal slip and solutal slip toward a stretching surface is pondered by Ibrahim and Shankar (2013) and established that the thermal boundary layer thickness reduces by augmenting the slip parameter. The difference between the fluid velocity of the wall and the velocity of the wall itself is directly proportional to shear stress and this proportional factor named as slip length. The slip boundary condition is given by $|u|_{wall} = l_s|\frac{\partial u}{\partial y}|$, where l_s represents the slip length Hak (2001). The behaviour of velocity slip $|u|_{wall} = \frac{2-\sigma_v}{\sigma_v}\lambda_0\frac{\partial u}{\partial y}$ and temperature jump $T_{wall} = \frac{2-\sigma_T}{\sigma_T}\left(\frac{2r}{r+1}\right)\frac{\lambda_0}{Pr}\frac{\partial T}{\partial y}$, σ_v and σ_T denote momentum accommodation and temperature accommodation coefficient are studied by Maxwell (1879) and Smoluchowski (1898). Khan *et al.* (2013) studied the impact of velocity and temperature jump slip conditions on double diffusive nanofluid past a vertical plate and found that the velocity field increases on the behalf of an improvement in the velocity slip parameter. Rahman and Eltayeb (2011) pondered the conduct of rarefied fluids flow over a wedge along with Smoluchowski temperature slip condition and came up with the conclusion that the temperature field abates owing to an augmentation in temperature slip parameter. The impact of Maxwell velocity and Smoluchowski temperature slip boundary condition on rarefied gas fluid moving over a wedge is investigated by Das *et al.* (2017).

Global Digital Central
ISSN: 2151-8629

Hayat *et al.* (2015) have scrutinized the impact of MHD on three dimensional nanofluid flow towards a stretching sheet embedded with Maxwell velocity slip boundary condition. This paper is extension of work done by Hayat *et al.* (2015) under the inclusion of various effects.

In the light of above mentioned study Das *et al.* (2017) and Hayat *et al.* (2015) specially , the purpose of current research is to explore the conduct of nonlinear thermal radiation, viscous and Ohmic dissipation, homogeneos/heterogenous reactions, Maxwell velocity and Smoluchowski temperature slip boundary conditions on three dimensional rarefied Carreau fluid past a stretching sheet. According to best of author's knowledge no work have been reported yet to study the impact of slip conditions along with nonlinear thermal radiation and homogeneos/heterogenous reactions on rarefied fluid flow over a three dimensional stretchable surface.

2. MATHEMATICAL FORMULATION

The physical model used to represent the time independent three dimensional incompressible Carreau fluid flow behaviour is shown in Fig. 1. A non-uniform magnetic field B_0 is executed vertical to the sheet and furthermore the induced magnetic field effectiveness is amitated by assuming the small Reynolds number. The surface coincides with the plane $z = 0$ and the flow is restrained in the region $z > 0$. Flow considered in the current problem is optically thick and temperature difference of the fluid flow is large, therefore Rosseland radiative heat flux is not linearized with the help of Taylor's series. The surface is also assumed to exhibit the velocity slip conditions. The stretching surface velocities acting along x -axis and y- axis are $U_w(x) = lx$ and $V_w(x) = my$. The Maxwell velocity slip Maxwell (1879) acting along x -axis and y- axis at the surface of the sheet are given $\frac{2-\sigma_v}{\sigma_v}\lambda_0\frac{\partial u}{\partial z}$ and $\frac{2-\sigma_v}{\sigma_v}\lambda_0\frac{\partial v}{\partial z}$. The Smoluchowski temperature slip length Smoluchowski (1898) represented by $\frac{2-\sigma_T}{\sigma_T}\left(\frac{2r}{r+1}\right)\frac{\lambda_0}{Pr}$ is also considered. The constitutive equation

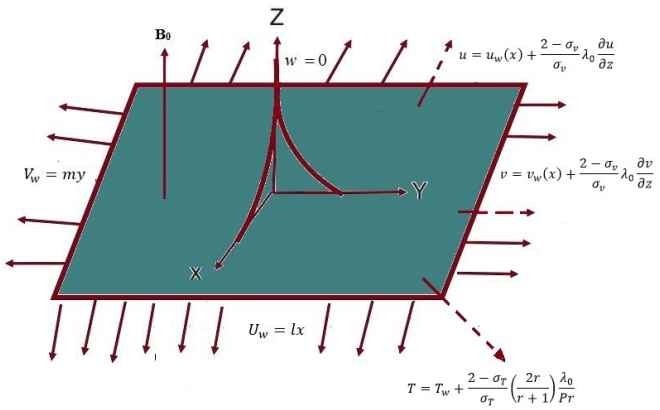

Fig. 1 Physical model of the problem.

of Carreau fluid is defined by

$$\tau = \mu_\infty + (\mu_0 - \mu_\infty)\left[1+\Gamma^2\dot{\gamma}^2\right]^{\frac{n-1}{2}}\dot{\gamma}, \tag{1}$$

The shear rate at zero and infinity is represented by μ_0 and μ_∞. Another important parameter n in the above equation represents the power-law index. The fluid exhibits the shear thickening behaviour for $n > 1$, shear thinning as $n < 1$ and furthermore Newtonian in the case $n = 1$. In the current formulation of the problem μ_∞ is considered as zero. Then the Carreau fluid equation reduces to

$$\tau = \mu_0\left[1+\Gamma^2\dot{\gamma}^2\right]^{\frac{n-1}{2}}\dot{\gamma}. \tag{2}$$

The apparent viscosity for Carreau fluid model can be expressed as

$$\mu = \mu_0\left[\beta^* + (1-\beta^*)\left[1+\Gamma^2\dot{\gamma}^2\right]^{\frac{n-1}{2}}\right], \tag{3}$$

The term $\beta^* = \frac{\mu_0}{\mu_\infty}$ represents the infinite shear-rate viscosity to the zero shear-rate viscosity and taken less than one in the current study. The homogeneous as well as the heterogeneous reaction between species A and B is premeditated byMansur *et al.* (2016). Cubic homogeneous chemical reaction is considered within the flow field whereas heterogeneous chemical reaction is taken at the catalyst surface. Homogeneous reaction is

$$A + 2B \to 3B, \quad rate = k_c ab^2, \tag{4}$$

heterogenous chemical reaction on the catalyst surface is premeditated by

$$A \to B, \quad rate = k_s a. \tag{5}$$

The concentration of chemical species A and B is established by the symbols a and b whereas the terms K_c and K_s represent the homogeneous as well as heterogeneous reaction rate constants. The governing nonlinear PDEs Khan *et al.* (2017a); Sajid *et al.* (2018); Mansur *et al.* (2016) are:

$$\frac{\partial u}{\partial x} + \frac{\partial v}{\partial y} + \frac{\partial w}{\partial z} = 0, \tag{6}$$

$$u\frac{\partial u}{\partial v} + v\frac{\partial u}{\partial y} + w\frac{\partial u}{\partial z} = \left(\beta^* + (1-\beta^*)\left(1+\Gamma^2\left(\frac{\partial u}{\partial z}\right)^2\right)^{\frac{n-1}{2}}\right)$$
$$\nu\frac{\partial^2 u}{\partial z^2} + \nu(n-1)(1-\beta^*)\Gamma^2\left(\frac{\partial u}{\partial z}\right)^2\frac{\partial^2 u}{\partial z^2}\left(1+\Gamma^2\left(\frac{\partial u}{\partial z}\right)^2\right)^{\frac{n-3}{2}} -$$
$$\frac{\sigma B_0^2}{\rho_f}u, \tag{7}$$

$$u\frac{\partial v}{\partial x} + v\frac{\partial v}{\partial y} + w\frac{\partial v}{\partial z} = \left(\beta^* + (1-\beta^*)\left(1+\Gamma^2\left(\frac{\partial v}{\partial z}\right)^2\right)^{\frac{n-1}{2}}\right)$$
$$\nu\frac{\partial^2 v}{\partial z^2} + \nu(n-1)(1-\beta^*)\Gamma^2\left(\frac{\partial v}{\partial z}\right)^2\frac{\partial^2 v}{\partial z^2}\left(1+\Gamma^2\left(\frac{\partial v}{\partial z}\right)^2\right)^{\frac{n-3}{2}} -$$
$$\frac{\sigma B_0^2}{\rho_f}v, \tag{8}$$

$$u\frac{\partial T}{\partial x} + v\frac{\partial T}{\partial y} + w\frac{\partial T}{\partial z} = \alpha_1\frac{\partial^2 T}{\partial z^2} + \frac{\sigma B_0^2}{\rho C_p}\left(u^2+v^2\right) - \frac{1}{\rho C_p}\frac{\partial q_r}{\partial z}, \tag{9}$$

$$u\frac{\partial a_1}{\partial x} + v\frac{\partial a_1}{\partial y} + w\frac{\partial a_1}{\partial z} = D_A\frac{\partial^2 a_1}{\partial z^2} - K_0 a_1 b_1^2, \tag{10}$$

$$u\frac{\partial b_1}{\partial x} + v\frac{\partial b_1}{\partial y} + w\frac{\partial b_1}{\partial z} = D_B\frac{\partial^2 b_1}{\partial z^2} - K_0 a_1 b_1^2. \tag{11}$$

The boundary conditions Mansur *et al.* (2016); Maxwell (1879); Smoluchowski (1898) associated with the above PDEs are

$$\left.\begin{aligned} &z = 0: \ u = lx + \frac{2-\sigma_v}{\sigma_v}\lambda_0\frac{\partial u}{\partial z}, \ v = my + \frac{2-\sigma_v}{\sigma_v}\lambda_0\frac{\partial v}{\partial z}, \\ &w = 0, \quad T = T_w + \frac{2-\sigma_T}{\sigma_T}\left(\frac{2r}{r+1}\right)\frac{\lambda_0}{Pr}, \\ &D_A\frac{\partial a_1}{\partial z} = K_s a_1, \quad D_B\frac{\partial b_1}{\partial z} = -K_s a_1. \\ &z \to \infty: \ u \to 0, v \to 0, T \to T_\infty, \ a_1 \to a_0, \ b_1 \to 0. \end{aligned}\right\} \tag{12}$$

The Rosseland approximation Mohamed and Wahed (2017) is defined as

$$q_r = -\frac{4\sigma^*}{3\kappa^*}\frac{\partial T^4}{\partial z} = -\frac{4\sigma^*}{3\kappa^*}T^3\frac{\partial T}{\partial z}. \tag{13}$$

Global Digital Central
ISSN: 2151-8629

The Stefan-Boltzmann and the mean absorption coefficients are expressed as σ^* and κ^* respectively.
By adopting the following similarity transformation Khan *et al.* (2017b),

$$\left.\begin{aligned} &u = lxf'(\eta),\ \ v = lyg'(\eta),\ \ w = -\sqrt{lv}\,(f(\eta)+g(\eta)),\\ &\theta(\eta) = \frac{T-T_\infty}{T_w-T_\infty},\ \ \eta = z\sqrt{\frac{l}{\nu}},\ \ h(\eta) = \frac{a_1}{a_0},\ \ q(\eta) = \frac{b_1}{a_0} \end{aligned}\right\} \tag{14}$$

Equations (6)-(10) get the following non-dimensional form:

$$f'''\left[(\beta^*+(1-\beta^*))\left(1+We_1^2f''^2\right)^{\frac{n-3}{2}}\left(1+nWe_1^2f''^2\right)\right] - \tag{15}$$
$$f'^2+f''(f+g)-Mf'=0,$$

$$g'''\left[(\beta^*+(1-\beta^*))\left(1+We_2^2g''^2\right)^{\frac{n-3}{2}}\left(1+nWe_2^2g''^2\right)\right] - \tag{16}$$
$$g'^2+g''(f+g)-Mg'=0,$$

$$\left[1+Rd\,(1+(\theta_w-1)\theta)^3\right]\theta''+3Rd\,(1+(\theta_w-1)\theta)^2(\theta_w-1)$$
$$\theta'^2+MP_r\left(Ec_xf'^2+Ec_yg'^2\right)+Pr\,(f+g)\,\theta'=0, \tag{17}$$

$$\frac{1}{Sc}h''+h'(f+g)-Khq^2=0, \tag{18}$$

$$\frac{\varphi}{Sc}q''+q'(f+g)+Khq^2=0. \tag{19}$$

The dimensionless form of the boundary conditions (11) is given below:

$$\left.\begin{aligned} \eta=0:\quad & f'(0)=1+\gamma f''(0),\ \ g'(0)=\beta+\gamma g''(0),\\ & \theta(0)=1+\delta\theta'(0),\ \ f(0)=0,\ \ g(0)=0,\\ & h'(0)=K_1h(0),\ \ \varphi q'(0)=-K_1h(0).\\ \eta\to\infty:\quad & f'\to0,\ g'\to0,\ \theta\to0,\ h\to1,\ q\to0. \end{aligned}\right\} \tag{20}$$

Various dimensionless parameters appearing in Equations (14)-(19) are characterized as

$$\left.\begin{aligned} &We_1=\Gamma^2\frac{l^3x^2}{\nu},\quad Pr=\frac{\nu}{\alpha},\quad M=\frac{\sigma B_0^2}{\rho l},\\ &We_2=\Gamma^2l\frac{m^2y^3}{\nu},\quad \mu=\rho\nu,\quad \varphi=\frac{D_B}{D_A},\\ &Rd=\frac{16\sigma^*T_\infty^3}{3k^*\kappa},\quad \theta_w=\frac{T_w}{T_\infty},\quad Sc=\frac{\nu}{D_A},\\ &\beta=\frac{m}{l},\quad K_1=\frac{K_ca_0^2}{l},\quad \gamma=\frac{2-\sigma_v}{\sigma_v}\lambda_0\sqrt{\frac{l}{v}},\\ &Ec_x=\frac{l^2x^2}{C_P(T_w-T_\infty)},\quad Ec_y=\frac{m^2y^2}{C_P(T_w-T_\infty)},\\ &\delta=\frac{2-\sigma_T}{\sigma_T}\left(\frac{2r}{r+1}\right)\frac{\lambda_0}{Pr}\sqrt{\frac{l}{v}},\quad K=\frac{K_s}{D_Aa_0}\sqrt{\frac{v}{l}}. \end{aligned}\right\} \tag{21}$$

By taking D_A=D_B =1 and $\delta=1$ Mansur *et al.* (2016)

$$h(\eta)+q(\eta)=1. \tag{22}$$

By using Equation (21) in Equation (17), we get

$$\frac{h''}{Sc}+h'(f+g)-Kh(1-h)^2=0, \tag{23}$$

subject to the boundary conditions

$$h'(0)=K_1h(0),\ h\to1\ as\ \eta\to\infty. \tag{24}$$

The heat transfer coefficient is given by

$$Nu_x=-\frac{x}{(T_w-T_\infty)}\left.\frac{\partial T}{\partial z}\right|_{z=0}+\frac{xq_r}{k(T_w-T_\infty)}\left|_{z=0}\right.. \tag{25}$$

The dimensionless form of the heat transfer coefficient is bestowed by

$$Nu_xRe_x^{-1/2}=-\left(1+Rd\left((\theta_w-1)\theta(0)\right)^3\right)\theta'(0). \tag{26}$$

The skin friction coefficients are

$$C_{fx}=\frac{\tau_{xz}}{\frac{1}{2}\rho_fU_w^2}\quad,\quad C_{fy}=\frac{\tau_{yz}}{\frac{1}{2}\rho_fU_w^2}, \tag{27}$$

where the terms τ_{xz} and τ_{yz} are given by

$$\left.\begin{aligned} \tau_{xz}&=\mu\frac{\partial u}{\partial z}\left[(\beta^*+(1-\beta^*))\left(1+\Gamma^2\left(\frac{\partial u}{\partial z}\right)^2\right)^{\frac{n-1}{2}}\right],\\ \tau_{yz}&=\mu\frac{\partial v}{\partial z}\left[(\beta^*+(1-\beta^*))\left(1+\Gamma^2\left(\frac{\partial v}{\partial z}\right)^2\right)^{\frac{n-1}{2}}\right]. \end{aligned}\right\} \tag{28}$$

The skin friction coefficients in the dimensionless form are formulated as:

$$\left.\begin{aligned} &\frac{1}{2}C_{fx}Re_x^{\frac{1}{2}}=(\beta^*+(1-\beta^*))f''(0)\left(1+We_1^2f''^2\right)^{\frac{n-1}{2}},\\ &\left(\frac{U_w}{2V_w}\right)C_{fy}Re_x^{\frac{1}{2}}=(\beta^*+(1-\beta^*))g''(0)\left(1+We_2^2g''^2\right)^{\frac{n-1}{2}}. \end{aligned}\right\} \tag{29}$$

3. SOLUTION METHODOLOGY

The nonlinear, non-dimensional Equations (14)-(16) and Equation (22) along with the boundary conditions (19) and (23) can be comprehended with the assistance of the shooting strategy Na (1979) utilizing the RK4 method. For numerical solution, the unbounded domain $[0,\infty)$ has been replaced by $[0,\eta_{max}]$ where η_{max} is a real number chosen in such a way that the solution doesn't show significant variations for $\eta>\eta_{max}$. It is observed that $\eta_{max}=7$ guarantees an asymptotic convergence for all the results presented in this article. For convenience in the choice of missing conditions and computational efficiency, first the momentum Equations (14)-(15) will be solved numerically by the shooting method. Later on, using f and g as known functions, the energy Equation (16) will be treated numerically. Finally the concentration equation will be solved by the same technique by using the available solution of Equations (14)-(15). The momentum equations have been converted into a system of first order ODEs signifying f by y_1, f' by y_2, f'' by y_3, g by y_4, g' by y_5, g'' by y_6, $y_2(0)$ by γ_1 and $y_5(0)$ by γ_2. The resulting system of equations is:

$$\left.\begin{aligned} y_1'&=y_2,\\ y_2'&=y_3,\\ y_3'&=\frac{[y_2^2-y_3\,(y_1+y_4)+My_2]}{(\beta^*+(1-\beta^*))\left(1+We_1^2y_3^2\right)^{\frac{n-3}{2}}\left(1+nWe_1^2y_3^2\right)},\\ y_4'&=y_5,\\ y_5'&=y_6,\\ y_6'&=\frac{[y_5^2-y_6\,(y_1+y_4)+My_5]}{(\beta^*+(1-\beta^*))\left(1+We_2^2y_6^2\right)^{\frac{n-3}{2}}\left(1+nWe_2^2y_6^2\right)}, \end{aligned}\right\} \tag{30}$$

with initial conditions are

$$\left.\begin{aligned} &y_1(0)=0,\ \ y_2(0)=1+\gamma\gamma_1,\ \ y_3(0)=\gamma_1,\ \ y_4(0)=0,\\ &y_5(0)=\beta+\gamma\gamma_2,\ \ y_6(0)=\gamma_2. \end{aligned}\right\} \tag{31}$$

To reach close enough to the missing initial conditions, Newton's method is iteratively applied until the following criteria is met.

$$\max\{|y_2(\eta_{max})|,|y_5(\eta_{max})|\}<\epsilon, \tag{32}$$

where ϵ depicts a small positive number.
In the case of temperature equation, the transformed ODE (16) is converted into first order ODEs by denoting θ by w_1, θ' by w_2. As a result of

the introduction of theses new variables, the following system of ODEs is achieved.

$$\left.\begin{aligned} w_1' &= w_2, \\ w_2' &= \frac{\left[\begin{array}{l} Pr(f+g)w_1 + MPr(Ec_x f'^2 + Ec_y g'^2) \\ +3Rd(1+(\theta_w-1)y_1)^2(\theta_w-1)w_2^2 \end{array}\right]}{-\left(1+Rd\left(1+(\theta_w-1)\,w_1\right)^3\right)}, \end{aligned}\right\} \tag{33}$$

with initial conditions

$$w_1(0) = 1+\delta\gamma_3 \quad , \quad w_2(0) = \gamma_3.$$

For the refinement of the initial guess γ_3, Newton's method is applied unless the condition underneath is fulfilled.

$$\max\{|w_1(\eta_{max}) - 0|\} < \epsilon. \tag{34}$$

The concentration equation (16) is converted into the first order ODEs by denoting h by z_1, h' by z_2. The first order ODEs are then given by:

$$\left.\begin{aligned} z_1' &= z_2, \\ z_2' &= Sc\left(-z_2\left(f+g\right) + Kz_1\left(1-z_1\right)^2\right), \end{aligned}\right\} \tag{35}$$

having initial conditions

$$z_1(0) = \gamma_4 \quad , \quad z_2(0) = K_1\gamma_4$$

For the improvement of the initial guess γ_4, the iterative scheme called Newton's method is used until the criteria given below is achieved.

$$\max\{|z_1(\eta_{max}) - 1|\} < \epsilon. \tag{36}$$

In Table 1, a comparison of the presently computed values of different physical quantities with those already published in literature.

Table 1 Comparison of $f''(0)$ for different values of β.

β	Irfan *et al.* (2018)	Hayat *et al.* (2015)	Present
0.1	1.01702	1.02026	1.02038
0.2	1.03458	1.03949	1.03958
0.3	1.05747	1.05795	1.05802
0.4	1.07052	1.07578	1.07583

4. RESULTS AND DISCUSSIONS

In the present section, the numerical solution of the dimensionless mathematical model has been presented and analyzed. The skin friction coefficient and $h'(0)$ against various parameters is delineated in Table 3 by keeping $Rd = 1$, $\theta_w = 1.5$, $Ec_x = 0.5$, $Ec_y = 0.5$, $Pr = 1$, $\delta = 1$ as fixed. According to Table 2, an enrichment in magnetic parameter M and the stretching rate parameter β prompts a decrease in the skin friction coefficient but an inverse behaviour is observed on account of the power-law index n (shear thickening) and the slip parameter γ. An improved behavior is seen in the skin friction coefficient along y-axis for the magnetic parameter M and the stretching rate β. However for n and γ a reverse behavior is experienced for skin friction coefficient. Table 3 demonstrates the behavior of the Nusselt number against different parameters, for fixed values of $We_1 = 0.1$, $We_2 = 0.1$, $Sc = 0.2$, $K = 2$,$K_1 = 1$. It is quite clear that boosting the values of n (shear thickening), the radiation parameters Rd, the temperature ratio parameter θ_w and Prandtl number Pr bring about an enlargement in the Nusselt number but situation is reverse on account of the remaining parameters like the magnetic parameter M, Eckert number Ec, stretching rate β, slip parameters γ and δ.

Figures 2-17 exhibit the behaviour of velocity, temperature and concentration profiles against various parameters arising in the present problem. Fig. 2 exhibits the dynamics of the velocity profiles f' and g' under the effect of the magnetic parameter M. It is noted that the magnetic field in the presence of electric current develops a force called Lorentz force which lessens the fluid velocity inside the boundary layer. Fig. 3 delineates the impact of the power-law index n on the velocity profiles f' and g'. The values of n have been taken for all the three cases shear thinning $n < 1$, shear thickening $n > 1$ and Newtonian $n = 1$. From this figure, it can be clearly seen that a boost in f' and g' happens due to an embellishment in the power-law index. An increment in the power law also guides to an improvement in the momentum boundary layer thickness. The impact of Weissenberg number We_1 on the velocity profile is manifested in Fig. 4. Weissenberg number is described as the ratio of the shear rate time to the relaxation time. Liquids turn out to be more thicker because of an augmentation in the Weissenberg number. Therefore velocity profile is reduced with an enrichment in the Weissenberg number. The execution of the velocity profile against the slip parameter γ is displayed in Fig. 5. Rising the values of the velocity slip over the stretching sheet lessens the fluid velocity. The impact of the Wessenberg number We_2 on the velocity profile is considered in Fig. 6. It is observed that the liquid turns out to be more viscous on the behalf of an amplification in the Weissenberg number which reduces the momentum boundary layer thickness and the velocity profile. Fig. 7 demonstrates the dynamics of the velocity field versus the slip parameter γ. The physical reason behind the velocity decrement is actually an increment in the frictional resistance existing between the surface and the fluid particles which reduces the fluid flow and the velocity profile. Fig. 8 displays the impact of the stretching parameter β on the velocity profile. An enlargement in the value of the stretching parameter brings about a diminishment in the velocity profile. Fig. 9 and Fig. 10 depicts the performance of viscosity ratio parameter β^* on the velocity profiles $f'(\eta)$ and $g'(\eta)$. It is quite cleat the fluid behaves like shear thickening on the behalf of an amplification in the β^* which reduces the fluid velocity and guides to a reduction in the velocity profiles. Fig. 11 displays the significant role of the frequently used parameter Prandtl number Pr, which is actually the ratio of the momentum diffusivity to the thermal diffusivity. It is well established that Prandtl number reduces the fluid temperature. Thermal diffusivity reduces for the larger values of Pr which guides to a thickness in the thermal boundary layer. Fig. 12 portrays the behavior of the velocity profile versus the Eckert number Ec_x. By boosting the Eckert number, more heat in the liquid is generated due to the frictional heating which improves the temperature behaviour. From Fig. 13, it is probed that by mounting the Eckert number Ec_y, an additional heat in the liquid is generated on account of the frictional force which is responsible for an augmentation in the temperature field. Fig. 14 demonstrates the effect of the magnetic parameter M on the temperature field. Lorentz force which is basically a drag force, causes a decrement in the fluid velocity which amplifies the temperature field. The behavior of radiation parameter Rd on the temperature profile is deliberated in Fig. 15 It is quite abvious that heightening the value of Rd escorts the temperature rise inside the boundary layer, and hence the temperature profile rises. Fig. 16 determines the impact of the temperature ratio parameter θ_w on the temperature profile. By ascending θ_w, an enlargement in the wall temperature is observed. As a result the temperature ratio parameter escalates and a rise in the temperature profile take place. Fig. 17 sketches the impact of the Schmidt number Sc on the concentration profile. When Schmidt number enhances, the viscous diffusion also increases which the concentration profile. The behavior of the concentration field against the homogeneous reaction parameter K is depicted in Fig. 18. The flow diffusivity fluctuates by mounting the value of the homogeneous reaction, which is the prominent factor for diminishment of the concentration profile. Fig. 19 examines the association between the heterogeneous reaction K_1 and the concentration field. An increment in the homogeneous reaction brings about a reduction in the concentration field.

Table 2 Values of momentum and concentration equations for various parameters.

M	n	β	γ	We_1	We_2	K	K_1	Sc	β^*	$\frac{1}{2}C_f Re_x^{\frac{1}{2}}$	$\frac{1}{2}C_f \frac{U_w}{V_w} Re_x^{\frac{1}{2}}$	$h'(0)$
0.1	0.5	0.5	0.3	0.1	0.1	2	1	0.2	0.1	-0.77771	-0.34821	0.06335
0.3										-0.82723	-0.37813	0.05855
0.5										-0.87228	-0.40461	0.05479
0.7										-0.91355	-0.42834	0.05178
	1									-0.77718	-0.34818	0.06337
	1.5									-0.77666	-0.34815	0.06339
	2									-0.77614	-0.34812	0.06340
		0.7								-0.78847	-0.52203	0.06849
		0.9								-0.80171	-0.70978	0.07343
		1.1								-0.81413	-0.90886	0.07823
			0.5							-0.64588	-0.29456	0.05891
			1							-0.46310	-0.21594	0.05206
			1.5							-0.36425	-0.17204	0.04798
				0.5						-0.75961	-0.34742	0.06302
				1						-0.72103	-0.34614	0.06214
				1.5						-0.67349	-0.34453	0.06104
					0.5					-0.77414	-0.34660	0.06331
					1					-0.77389	-0.34269	0.06319
					1.5					-0.77349	-0.33658	0.06299
						2.2				-0.77422	-0.34790	0.05362
						2.4				-0.77422	-0.34790	0.04527
						2.6				-0.77422	-0.34790	0.03822
							1.2			-0.77422	-0.34790	0.06694
							1.4			-0.77422	-0.34790	0.06979
							1.6			-0.77422	-0.34790	0.07212
								0.6		-0.77422	-0.34790	0.03465
								0.7		-0.77422	-0.34790	0.03964
								0.8		-0.77422	-0.34790	0.05451
									0.2	-0.77416	-0.34789	0.05452
									0.3	-0.77410	-0.34789	0.05454
									0.4	-0.77405	-0.34789	0.05455

Table 3 Effects of different physical parameters on Nu_x.

M	n	Rd	θ_w	Ec_x	Ec_y	Pr	β	γ	δ	$Nu_x Re_x^{\frac{-1}{2}}$
0.1	0.5	1	0.5	0.5	0.5	1	0.5	0.3	1	0.34080
0.3										0.30183
0.5										0.26786
0.7										0.23795
	1									0.34086
	1.5									0.34092
	2									0.34098
		1.2								0.35218
		1.4								0.36356
		1.6								0.37495
			1							0.43589
			1.5							0.58527
			2							0.77819
				0.7						0.30118
				0.9						0.26196
				1.1						0.22313
					0.7					0.33103
					0.9					0.32128
					1.1					0.31155
						1.2				0.36337
						1.4				0.38293
						1.6				0.39986
							0.7			0.33602
							0.9			0.32090
							1.1			0.29619
								0.5		0.35229
								0.7		0.35673
								0.9		0.35774
									1.2	0.32066
									1.4	0.30303
									1.6	0.28744

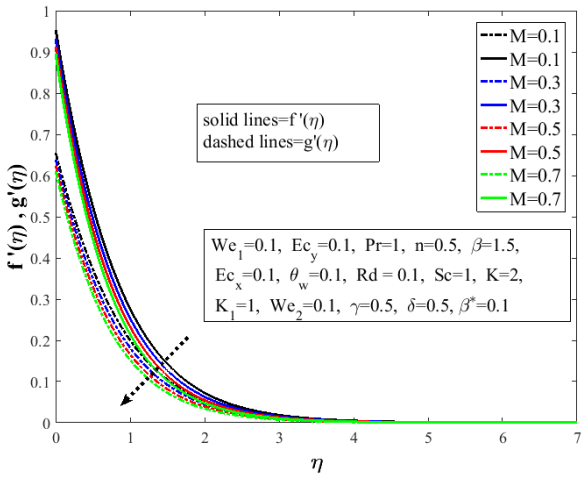

Fig. 2 Impact of M on f' and g'.

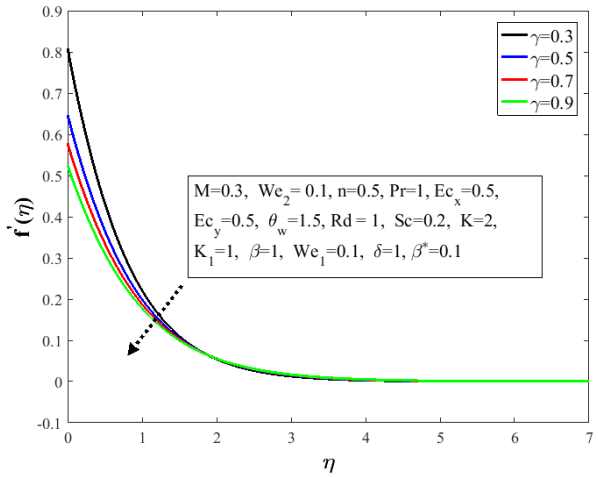

Fig. 5 Influence of γ on f'.

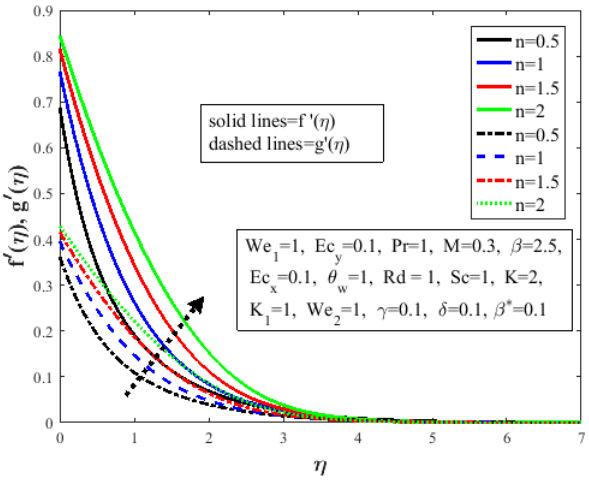

Fig. 3 Effect of n on f' and g'.

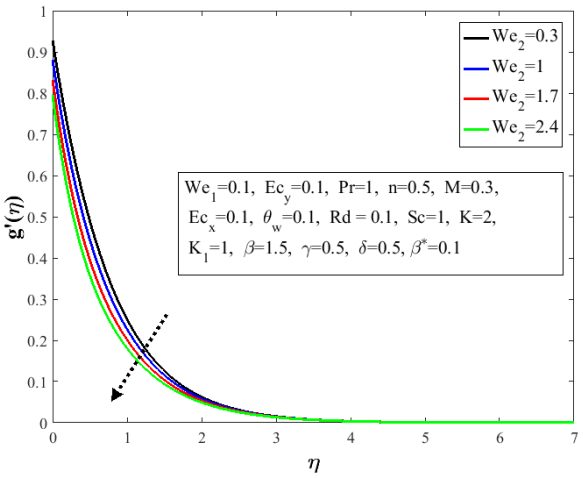

Fig. 6 Influence of We_2 on g'.

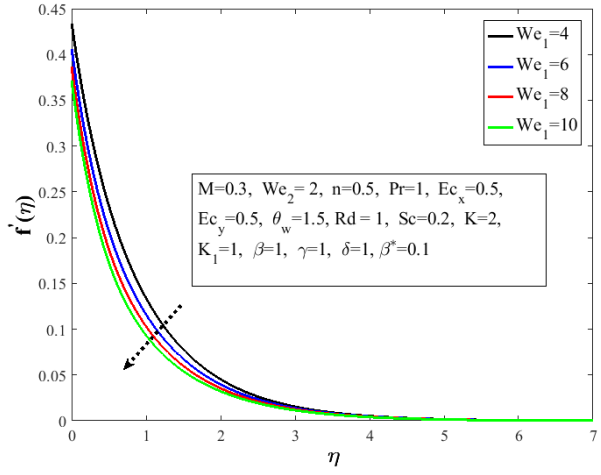

Fig. 4 Influence of We_1 on f'.

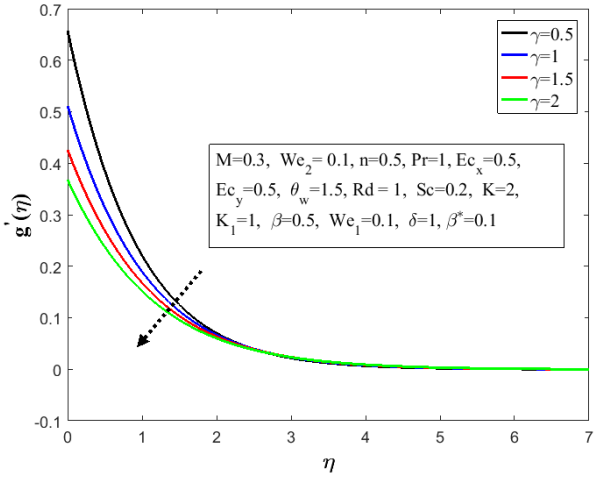

Fig. 7 Influence of γ on g'.

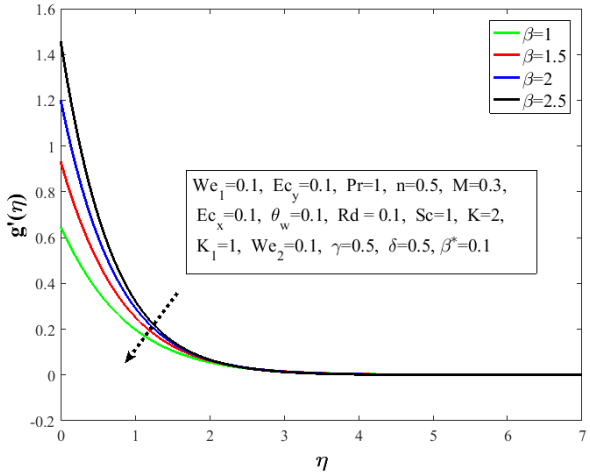

Fig. 8 Influence of β on g'.

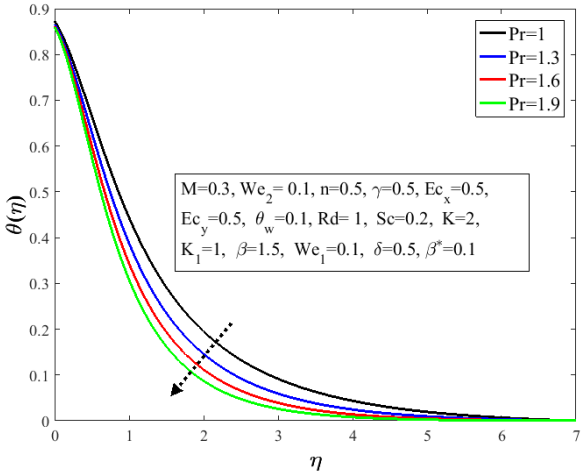

Fig. 11 Effect of Pr on θ.

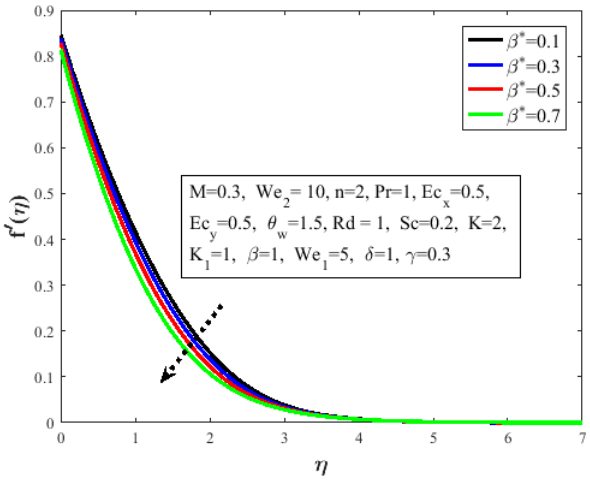

Fig. 9 Influence of β^* on f'.

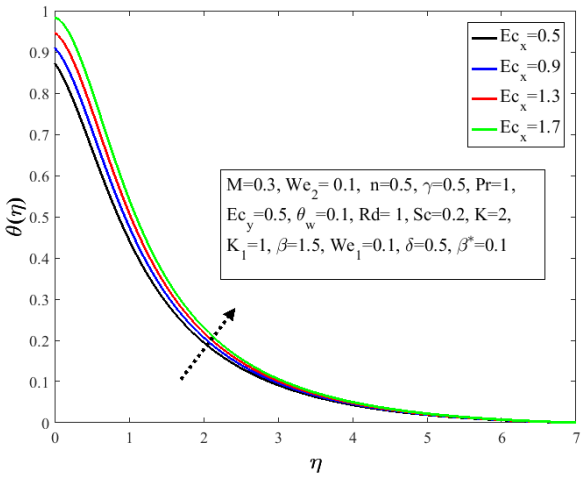

Fig. 12 Influence of Ec_x on θ.

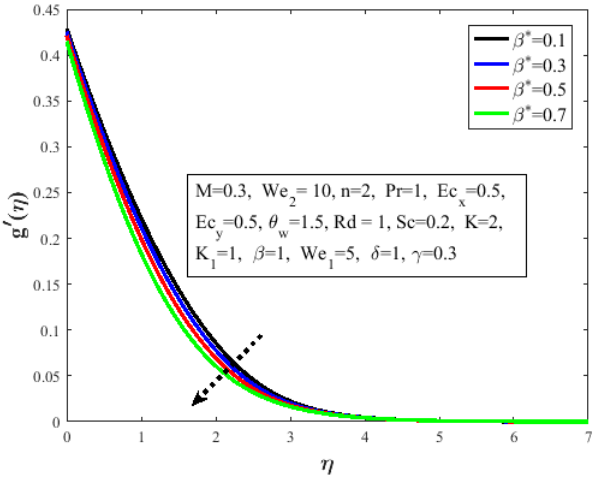

Fig. 10 Influence of β^* on g'.

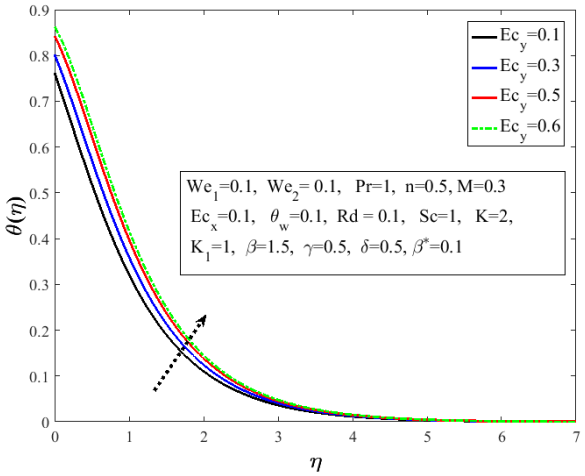

Fig. 13 Influence of Ec_y on θ.

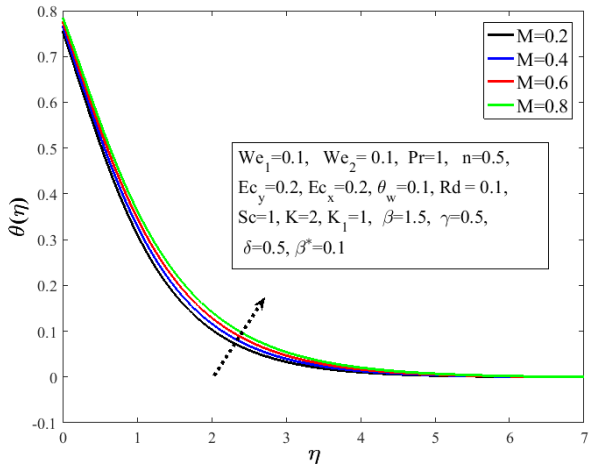

Fig. 14 Impact of M on θ.

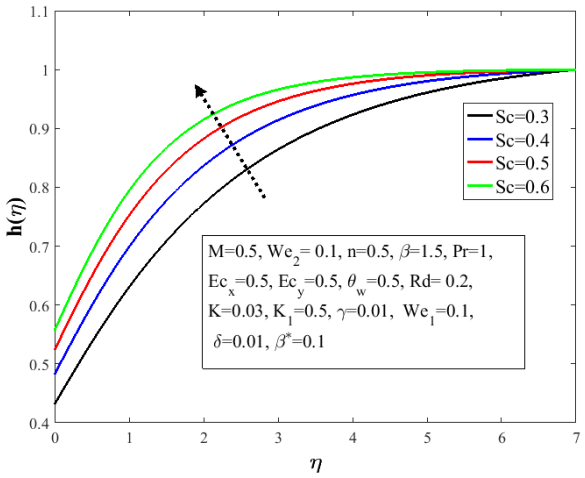

Fig. 17 Effect of Sc on h.

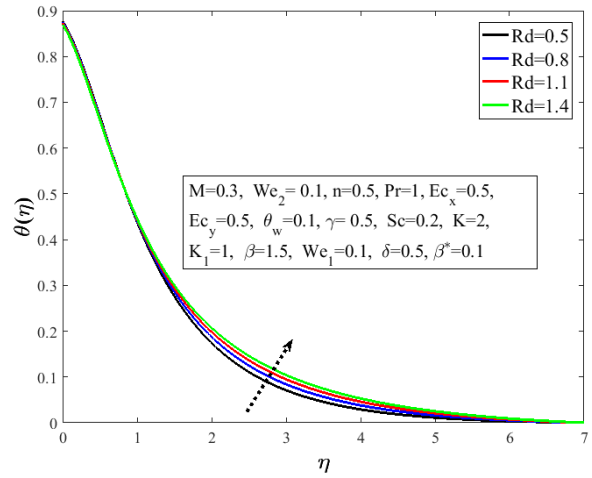

Fig. 15 Impact of Rd on θ.

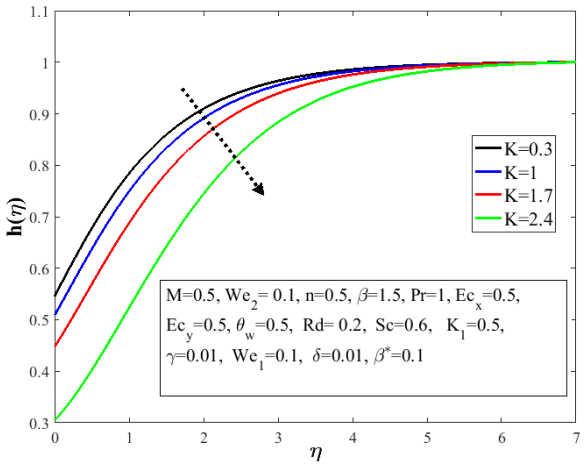

Fig. 18 Effect of K on h.

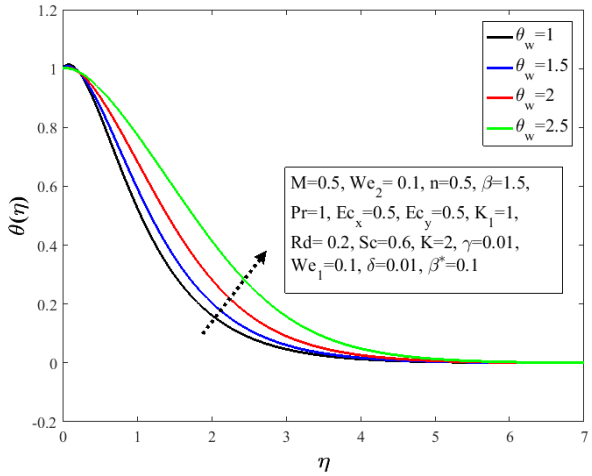

Fig. 16 Effect of θ_w on θ.

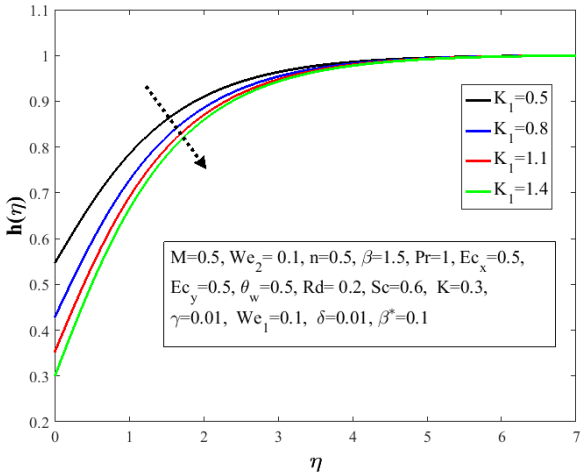

Fig. 19 Effect of K_1 on h.

5. FINAL REMARKS

A three dimensional Carreau fluid flow past a stretching sheet along with different effects like viscous dissipation, homogeneous/heterogeneous reaction, Ohmic dissipation, velocity slips, temperature slip, nonlinear thermal radiation is analyzed. The shooting method is utilized to solve the system of nonlinear ordinary differential equations. Some decisive comments from the concluding work are as below:

- The temperature profile increases with an increment in the Eckert number Ec_x along x-axis and Ec_y along y-axis.
- By enhancing the Weissenberg numbers We_1 and We_2, a decrement in the velocity profiles is prompted.
- The temperature profile depicts an enhancing behavior for the magnetic parameter M and the Schmidt number Sc.
- The velocity profiles $f'(\eta)$ and $g'(\eta)$ are decreased for the higher values of the velocity slip parameter..
- A decay in the concentration profile is observed for the larger values of the homogeneous reaction parameter K.
- The concentration field depreciates in the case of an enrichment in the heterogeneous reaction parameter K_1
- The concentration profile depreciates as a result of an augmentation in the homogeneous and heterogeneous reactions.

6. DATA AVAILABILITY

The data supporting the findings of this study are available within the article.

7. CONFLICTS OF INTEREST

The author(s) declare(s) that there is no conflict of interest regarding the publication of this paper.

8. ARTICLE FUNDING

The corresponding author pay article processing charges.

NOMENCLATURE

We_1	Weissenberg number along $x-axis$
We_2	Weissenberg number along $y-axis$
C_∞	ambient concentration
D_A	Thermal diffusion coefficient
D_B	Brownian diffusion coefficient
Ec_x	Eckert number along $x-axis$
Ec_y	Eckert number along $y-axis$
M	Magnetic parameter
n	Power-law index
T	temperature (K)
u, v	velocity components (m/s)
x, y	coordinates along and normal to stretching surface (m)
Rd	Radiation parameter
θ_w	temperature ratio parameter
c_p	specific heat at constant pressure $(J/Kg.K)$
Sc	Schmidt number
Nu_x	Nusselt number
Pr	Prandtl number
K_1	strength of heterogeneous reaction
K	strength of homogeneous reaction
T_∞	ambient temperature
T_w	wall temperature
U_w, V_w	stretching velocities (m/s)
r	specific heat ratio
l_s	slip length (m)
q_w	surface heat flux
q_r	surface heat flux
Greek Symbols	
Γ	relaxation time
ρ	density of fluid (Kg/m^3)
η	similarity variable
ϕ	field concentration
μ	dynamic viscosity $(Kg/m.s)$
ν	kinematic viscosity (m^2/s)
σ^*	Stefan-Boltzman constant$(5.67 \times 10^{-8} W/m^2.K^4)$
k^*	mean absorption coefficient
φ	ratio of diffusion coefficients
γ	velocity slip parameter
δ	temperature jump
$\dot{\gamma}$	deformation rate
λ_0	molecular mean free path
κ	thermal conductivity $(W/m.K)$
α_1	thermal diffusivity (m^2/s)
σ_υ	momentum accomodation coefficient
σ_T	temperature accomodation coffecient

REFERENCES

Ali, M.E., and Sandeep, N., 2017, "Cattaneo-Christov model for radiative heat transfer of magnetohydrodynamic Casson-Ferrofluid: A numerical study," *Results in Physics*, **7**, 21–30.
https://dx.doi.org/10.1016/j.rinp.2016.11.055.

Aljoufi, M.D., and Ebaid, A., 2016, "Effect of a convective boundary condition on boundary layer slip flow and heat transfer over a stretching sheet in view of the exact solution," *Journal of Theoretical and Applied Mechanics*, **46**(4), 85–95.
https://dx.doi.org/10.1515/jtam-2016-0022.

Astuti, H., Srib, P., and Kaprawi, S., 2019, "Natural convection of nanofluids past an accelerated vertical plate with variable wall temperature by presence of the radiation," *Frontiers in Heat and Mass Transfer*, **13**, 3.
http://dx.doi.org/10.5098/hmt.13.3.

Azam, M., Khan, M., and Alshomrani, A.S., 2017, "Unsteady radiative stagnation point flow of MHD Carreau nanofluid over expanding/contracting cylinder," *International Journal of Mechanical Sciences*, **130**, 64–73.
https://dx.doi.org/10.1016/j.ijmecsci.2017.06.010.

Bachok, N., Ishak, A., and Pop, I., 2011, "On the stagnation-point flow towards a stretching sheet with homogeneous/heterogeneous reaction effects," *Communications in Nonlinear Science and Numerical Simulation*, **16**(11), 4296–4302.
https://dx.doi.org/10.1016/j.cnsns.2011.01.008.

Bilal, M., Sagheer, M., Hussain, S., and Mehmood, Y., 2017, "MHD Stagnation Point Flow of Williamson Fluid over a Stretching Cylinder with Variable Thermal Conductivity and Homogeneous/Heterogeneous Reaction," *Communications in Theoretical Physics*, **67**(6), 688–696.
https://dx.doi.org/10.1088/0253-6102/67/6/688.

Chaudhary, M.A., and Merkin, J.H., 1995, "A simple isothermal model for homogeneous/heterogeneous reactions in boundary-layer flow. I Equal diffusivities," *Fluid Dynamics Research*, **16**(6), 311–333.
https://dx.doi.org/10.1016/0169-5983(95)00015-6.

Cortell, R., 2011, "Suction, viscous dissipation and thermal radiation effects on the flow and heat transfer of a power-law fluid past an infinite porous plate," *Chemical Engineering Research and Design*, **89**(1), 85–93.
https://dx.doi.org/10.1016/j.cherd.2010.04.017.

Cortell, R., 2014, "Fluid flow and radiative nonlinear heat transfer over a stretching sheet," *Journal of King Saud University – Science*, **26**(2), 161–167.
https://dx.doi.org/10.1016/j.jksus.2013.08.004.

Das, K., Sharma, R.P., and Duari, P.R., 2017, "Hydromagnetic rarefied fluid flow over a wedge in the presence of surface slip and thermal radiation," *Int J of Applied Mechanics and Engineering*, **22**(4), 827–837.
https://dx.doi.org/ 10.1515/ijame-2017-0054.

Devakar, M., Sreenivasu, D., and Shankar, B., 2014, "Analytical solutions of coupled stress fluid flows with slip boundary conditions," *Alexandria Engineering Journal*, **53**(3), 723–730.
https://dx.doi.org/10.1016/j.aej.2014.06.005.

Fang, T., Zhang, J., and Yao, S., 2009, "Slip MHD viscous flow over a stretching sheet: an exact solution," *Communications in Nonlinear Science and Numerical Simulation*, **14**(11), 3731–3737.
https://dx.doi.org/10.1016/j.cnsns.2009.02.012.

Ghiasi, E.K., and Saleh, R., 2019, "2D flow of Casson fluid with non-uniform heat source/sink and Joule heating," *Frontiers in Heat and Mass Transfer*, **12**, 4.
http://dx.doi.org/10.5098/hmt.12.4.

Gireesha, B.J., Kumar, P.B.S., Mahanthesh, B., Shehzad, S.A., and Rauf, A., 2017, "Nonlinear 3D flow of Casson-Carreau fluids with homogeneous-heterogeneous reactions: A comparative study," *Results in Physics*, **7**, 2762–2770.
https://dx.doi.org/10.1016/j.rinp.2017.07.060.

Hak, M.G., 2001, "Flow physics in MEMS Physique des ecoulements dans les MEMS," *Mecanique and Industries*, **2**(4), 313–341.
http://www.sciencedirect.com/science/article/pii/S1296213901011125.

Hayat, T., Aziz, A., Muhammad, T., and Alsaedi, A., 2017, "Three-dimensional flow of nanofluid with heat and mass flux boundary conditions," *Chinese Journal of Physics*, **55**(4), 1495–1510.
https://dx.doi.org/10.1016/j.cjph.2017.05.005.

Hayat, T., Imtiaz, M., Alsaedi, A., and Kutbi, M.A., 2015, "MHD three-dimensional flow of nanofluid with velocity slip and nonlinear thermal radiation," *Journal of Magnetism and Magnetic Materials*, **396**, 31–37.
https://dx.doi.org/10.1016/j.jmmm.2015.07.091.

Ibrahim, W., and Shankar, B., 2013, "MHD boundary layer flow and heat transfer of a nanofluid past a permeable stretching sheet with velocity, thermal and solutal slip boundary conditions," *Computers and Fluids*, **75**, 1–10.
https://dx.doi.org/10.1016/j.compfluid.2013.01.014.

Irfan, M., Khan, M., and Khan, W.A., 2018, "Interaction between chemical species and generalized Fourier's law on 3D flow of Carreau fluid with variable thermal conductivity and heat sink/source: A numerical approach," *Results in Physics*, **10**, 107–117.
https://dx.doi.org/10.1016/j.rinp.2018.04.036.

Jyothi, K., and Reddy, P.S.R.M.S., 2019, "Physical aspects of shear thinning/thickening behavior in radiative flow of magnetite Carreau nanofluid with nanoparticle mass flux conditions," *Journal of the Brazilian Society of Mechanical Sciences and Engineering*, **41**, 415.
https://doi.org/10.1007/s40430-019-1904-7.

Kameswaran, P.K., Shaw, S., Sibanda, P., and Murthy, P.V.S.N., 2013, "Homogeneous/heterogeneous reactions in a nanofluid flow due to a porous stretching sheet," *International Journal of Heat and Mass Transfer*, **57**(2), 465–472.
https://dx.doi.org/10.1016/j.ijheatmasstransfer.2012.10.047.

Khan, M., Irfan, M., and Khan, W.A., 2017a, "Numerical assesment of solar energy aspects on 3D magneto Carreau nanofluid: A revised proposed relation," *International Journal of Hydrogen Energy*, **42**(34), 22054–22065.
https://dx.doi.org/10.1016/j.ijhydene.2017.07.116.

Khan, M., Irfan, M., Khan, W.A., and Alshomrani, A.S., 2017b, "A new modeling for 3D Carreau fluid flow considering nonlinear thermal radiation," *Results in Physics*, **7**, 2692–2704.
https://dx.doi.org/10.1016/j.rinp.2017.07.024.

Khan, M., Irfan, M., Khan, W.A., and Ayaz, M., 2018, "Aspects of improved heat conduction relation and chemical processes in 3D Carreau fluid flow," *Pramana*, **91**, 14.
https://dx.doi.org/10.1007/s12043-018-1579-0.

Khan, W.A., Uddin, M.J., and Ismail, A.I.M., 2013, "Hydrodynamic and thermal slip effect on doublediffusive free convective boundary layer flow of a nanofluid past a flat vertical plate in the moving free stream," *PLOS one*, **8**, e54024.
https://dx.doi.org/10.1371/journal.pone.0054024.

Krishnamurthy, M.R., Prasannakumara, B.C., Gorla, R.S.R., and Gireesha, B.J., 2016, "Non-Linear Thermal Radiation and Slip Effect on Boundary Layer Flow and Heat Transfer of Suspended Nanoparticles Over a Stretching Sheet Embedded in Porous Medium with Convective Boundary Conditions," *Journal of Nanofluids*, **5**(4), 1–9.
https://dx.doi.org/10.1166/jon.2016.1238.

Liu, I.C., and Andersson, H.I., 2008, "Heat transfer over a bidirectional stretching sheet with variable thermal conditions," *International Journal of Heat and Mass Transfer*, **51**, 4018–4024.
https://dx.doi.org/10.1016/j.ijheatmasstransfer.2007.10.041.

Machireddy, G.R., and Naramgari, S., 2018, "Heat and mass transfer in radiative MHD Carreau fluid with cross diffusion," *Ain Shams Engineering Journal*, **9**, 1189–1204.
https://doi.org/10.1016/j.asej.2016.06.012.

Magyari, E., and Pantokratoras, A., 2011, "Note on the effect of thermal radiation in the linearized Rosseland approximation on the heat transfer characteristics of various boundary layer flows," *International Communications in Heat and Mass Transfer*, **38**(5), 554–556.
https://dx.doi.org/10.1016/j.icheatmasstransfer.2011.03.006.

Mahanthesha, B., Gireesha, B.J., and Gorla, R.S.R., 2016, "Nonlinear radiative heat transfer in MHD three-dimensional flow of water based nanofluid over a non-linearly stretching sheet with convective boundary condition," *Journal of the Nigerian Mathematical Society*, **35**(1), 178–198.
https://dx.doi.org/10.1016/j.jnnms.2016.02.003.

Mansur, S., Ishak, A., and Pop, I., 2016, "MHD Homogeneous-Heterogeneous Reactions in a Nanofluid due to a Permeable Shrinking Surface," *Journal of Applied Fluid Mechanics*, **9**(3), 1073–1079.
https://dx.doi.org/10.18869/acadpub.jafm.68.228.23044.

Maxwell, J.C., 1879, "On stresses in rarefied gases arising from inequalities of temperature," *Philosophical Transactions of the Royal Society of London*, **170**(189), 231–256.
https://dx.doi.org/10.1098/rspl.1878.0052.

Megahed, A.M., 2019, "Carreau fluid flow due to nonlinearly stretching sheet with thermal radiation, heat flux, and variable conductivity," *Applied Mathematics and Mechanics (English Edition)*, **40**, 1615–1624. https://doi.org/10.1007/s10483-019-2534-6.

Merkin, J.H., 1996, "A model for isothermal homogeneous-heterogeneous reactions in boundary-layer flow," *Mathematical and Computer Modelling*, **26**(8), 125–136. https://dx.doi.org/10.1016/0895-7177(96)00145-8.

Misra, J.C., and Adhikary, S.D., 2017, "Flow of a Bingham fluid in a porous bed under the action of a magnetic field: Application to magneto-hemorheology," *Engineering Science and Technology, an International Journal*, **20**(3), 973–981. https://dx.doi.org/10.1016/j.jestch.2016.11.008.

Mohamed, S., and Wahed, A., 2017, "Nonlinear Rosseland thermal radiation and magnetic field effects on flow and heat transfer over a moving surface with variable thickness in a nanofluid," *Canadian Journal of Physics*, **95**, 267–273. https://dx.doi.org/10.1139/cjp-2016-0345.

Mukhopadhyay, S., Mondal, I.C., and Chamkha, A.J., 2013, "Casson Fluid Flow and Heat Transfer Past a Symmetric Wedge," *Heat Transfer:Asian Research*, **42**(8), 665–757. https://dx.doi.org/10.1002/htj.21065.

Na, T.Y., 1979, *Computational methods in engineering boundary value problems*, Academic Press, NY, U.S.A.

Nagalakshm, P.S.S., and Vijaya, N., 2020, "MHD flow of Carreau nanofluid explored using CNT over a nonlinear stretched sheet," *Frontiers in Heat and Mass Transfer*, **14**, 4. http://dx.doi.org/10.5098/hmt.14.4.

Nandkeolyar, R., Kameswaran, P.K., Shaw, S., and Sibanda, P., 2014, "Heat transfer on nanofluid flow with homogeneous-heterogeneous reactions and internal heat generation," *Journal of Heat Transfer*, **136**(12), 122001. https://dx.doi.org/10.1115/1.4028644.

Narayana, M., Titus, L.S.R., Abraham, A., and Sibanda, P., 2014, "Modelling micropolar ferromagnetic fluid flow due to stretching of an elastic sheet," *Afrika Matematika*, **25**, 667–679. https://dx.doi.org/10.1007/s13370-013-0145-7.

Olajuwon, B.I., 2011, "Convection heat and mass transfer in a hydromagnetic Carreau fluid past a vertical porous plate in presence of thermal radiation and thermal diffusion," *Thermal science*, **15**, 241–252. https://dx.doi.org/10.2298/TSCI101026060O.

Rahman, M.M., and Eltayeb, I.A., 2011, "Convective slip flow of rarefied fluids over a wedge with thermal jump and variable transport properties," *International Journal of Thermal Sciences*, **50**(4), 468–479. https://dx.doi.org/10.1016/j.ijthermalsci.2010.10.020.

Raju, C.S.K., Ibrahim, S.M., Anuradha, S., and Priyadharshini, P., 2016, "Bio-convection on the nonlinear radiative flow of a Carreau fluid over a moving wedge with suction or injection," *The European Physical Journal Plus*, **131**, 409. https://doi.org/10.1140/epjp/i2016-16409-7.

Raju, C.S.K., and Sandeep, N., 2016, "Unsteady three-dimensional flow of Casson–Carreau fluids past a stretching surface," *Alexandria Engineering Journal*, **55**(2), 1115–1126. https://doi.org/10.1016/j.aej.2016.03.023.

Sajid, T., Sagheer, M., Hussain, S., and Bilal, M., 2018, "DarcyForchheimer flow of Maxwell nanofluid flow with nonlinear thermal radiation and activation energy," *AIP Advances*, **8**, 035102. https://dx.doi.org/10.1063/1.5019218.

Shateyi, S., and Muzara, H., 2020, "Unsteady MHD Blasius and Sakiadis flows with variable thermal conductivity in the presence of thermal radiation and viscous dissipation," *Frontiers in Heat and Mass Transfer*, **14**, 18. http://dx.doi.org/10.5098/hmt.14.18.

Sivasankaran, S., Niranjan, H., and Bhuvaneswari, M., 2017, "Chemical reaction, radiation and slip effects on MHD mixed convection stagnation-point flow in a porous medium with convective boundary condition," *International Journal of Numerical Methods for Heat and Fluid Flow*, **27**, 454–470. https://dx.doi.org/10.1108/HFF-02-2016-0044.

Smoluchowski, M., 1898, "Ueber warmeleitung in verdunnten gasen," *Annalen der Physik*, **64**(1), 101–130. https://dx.doi.org/10.1002/andp.18983000110.

Turkyilmazoglu, M., 2014, "Three dimensional MHD flow and heat transfer over a stretching/shrinking surface in a viscoelastic fluid with various physical effects," *International Journal of Heat and Mass Transfer*, **78**, 150–155. https://dx.doi.org/10.1016/j.ijheatmasstransfer.2014.06.052.

Xinhui, S., Li, H., Shen, Y., and Zheng, L., 2017, "Effects of nonlinear velocity slip and temperature jump on pseudo-plastic power-law fluid over moving permeable surface in presence of magnetic field," *Applied Mathematics and Mechanics*, **38**, 333–342. https://dx.doi.org/10.1007/s10483-017-2178-8.

Zheng, L., Niu, J., Zhang, X., and Gao, Y., 2012, "MHD Flow and Heat Transfer over a porous shrinking surface with velocity slip and temperature jump," *Mathematical and Computer Modeling*, **56**(6), 133–144. https://dx.doi.org/10.1016/j.mcm.2011.11.080.

Ziabakhsh, Z., Domairry, G., Bararnia, H., and Babazadeh, H., 2010, "Analytical solution of flow and diffusion of chemically reactive species over a nonlinearly stretching sheet immersed in a porous medium," *Journal of the Taiwan Institute of Chemical Engineers*, **41**(1), 22–28. https://dx.doi.org/10.1016/j.jtice.2009.04.011.